



CHAPTER 1

INTRODUCTION

The major aim of geophysical fluid dynamics is the study of large scale motions on the Earth and other planets of the solar system. In a continuous kinetic energy spectrum, large scales usually contain more energy than small scales. Mid-latitude westerlies, meandering jet streams and banded zonal flows in oceans in the Earth system, banded flow patterns and great red spot of Jupiter and banded flow pattern of Saturn are prominent examples. Understanding of Generation mechanism of the large scale phenomena is still ongoing research topic in geophysical fluid dynamics. Geophysical flows are characterized by a continuous spectrum of kinetic energy encompassing several orders of magnitude of spatial and temporal scales of motion. Usually energy of large scales of motion is transferred to the small scales. However, an inverse cascade of energy from small to large scales is possible as well due to nonlinearity. This work aims to contribute to the basic understanding of generation of large scale phenomena.

Fluid layers of planets, e.g., atmosphere, ionized gases in stars, liquid core, subsurface oceans, are characterized by rotational and convective motions. Many researchers focused only on the convective motions to study generation of the large scale motions and assume that rotation play a minor role (Le Bars et al. 2015). However, recent studies (Dwyer et al. 2011; Le Bars et al. 2011; Stanley et al. 2005) suggested that other kinds of forcings such as rotation play a role in organizing the large scale structures in the planets and stars. Different forces and mechanisms are relevant in such systems and sometimes it is difficult to identify the relation between a mechanism and phenomenon. Complexity of the system can be substantially reduced, considering an idealized system which takes into accounts only one of the forcings. A deep understanding of the mechanism and phenomenon can be gained in this way. We concentrate on the effect of rotation.

Rotation of solar objects is a necessary source for fluid flows in liquid layers. Many Planets and satellites in the solar system undergo harmonic variations in their rotation period due to mechanical forcings such as tidal forcing, precession/nutation and libration in longitude. As stated by Le Bars et al. (2015), these mechanical harmonic forcings do not provide the energy to derive the large scale motions, instead similar to a conveyor they extract some part of the rotational energy and convert it into fluid motions. Resonant



excitation of inertial waves (inertial normal modes and wave attractors) and occurrence of instabilities such as centrifugal (rotational) are examples of this energy transfer.

Focus of the current work is on the longitudinal libration. This is motivated by the opportunity of realization of this type of forcing in a laboratory experiment. Nevertheless, the discussion might be generalized to other mechanical forcings. Longitudinal libration is a time periodic variation of the rotation rate of a planet around its axis of symmetry. It is reported that longitudinal libration exists on Mercury, Earth's Moon, Mars' moons, Phobos and Deimos, four moons of Jupiter and many moons of Saturn (Yoder 1995; Comstock and Bills 2003; Noir et al. 2009). One of the key questions is how librational forcing couples with the interior fluid layers of the planet deriving large scale motions.

The current work tries to fill the existing gap in understanding of generation of the zonal mean flow as a large scale structure. The main focus is on the following mechanisms:

- 1- Mean flow generation by resonant excitation of inertial waves, forming normal modes and wave attractors.
- 2- Mean flow generation by intermittent centrifugal (rotational) instability.

These mechanisms are also relevant for other mechanical forcings such as tidal and precession/nutation, thus the discussion might be applied for them as well. In the following we summarize what is known about the two mechanisms, and introduce open questions.

Mechanism 1:

A prominent example of inertial waves in the Earth's atmosphere and oceans is the well known near-inertial waves (Plougonven and Snyder 2007; Shakespeare and Taylor 2014) which play a major role in energy transfer. Another example is when the Earth's rotation is slightly perturbed by large deep earthquakes and inertial waves are resonantly excited in the Earth's core (Melchior and Ducarme 1986; and Aldridge and Lumb 1987). Existence of the inertial waves is not restricted to the Earth. Dintrans and Ouyed (2001) and Wu (2005 a and b) reported the excitation of inertial normal modes on the Jupiter. Savonije and Papaloizou (1997) and Papaloizou and Savonije (1997) reported that inertial normal modes can be excited in adiabatic convective cores of high-mass stars. Papaloizou and Pringle (1981) investigated the excitation of inertial normal mode in close binary system in circular orbit.

Aiming to better understand inertial wave dynamics, many authors investigated formation of inertial normal modes and wave attractors by laboratory experiments and/or numerical simulations using idealized configurations; sphere (Aldridge and Toomre 1969; Sauret et al. 2013; Zhang et al. 2013), spherical shells (Tilgner 2007; Noir et al. 2009; Calkins et al. 2010; Koch et al. 2013; Sauret and Le Dizès 2013), cylinders (Noir et al. 2010; Swart et al. 2010; Lopez and Marques 2011, 2014; Sauret et al. 2012), cones (Beardsley 1970), prisms (Maas 2001) and boxes (Boisson et al. 2012).

The studies mentioned in the previous paragraph are devoted to the excitation of inertial waves. Only a few studies dealt with the generation of zonal mean flow as large scale motion by inertial waves. Tilgner (2007) showed that nonlinear self interaction of inertial waves along the attractor path leads to a zonal mean flow. Morize et al. (2010) confirmed



Tilgner's results using laboratory experiments. Inertial waves along the attractor path and inertial normal modes have different spatial structures, although both are characteristics of the system at resonance. The former is a progressive wave which appears as localized shear layer while the latter is a standing wave emerging as global cells (Boisson et al. 2012). The current work considers a system comprised of the two at the same time and contributes to clarifications of zonal mean flow generation mechanism.

Mechanism 2:

The discussion of centrifugal instability in a librational system dates back to early work of Aldridge and Toomre (1969). They showed experimentally formation of longitudinal roll structures in a centrifugally unstable boundary layer which is excited by longitudinal libration of a spherical container. These rolls are later called Görtler vortices by Noir et al. (2009) and Noir et al. (2010). They are also similar to those found by Görtler (1955) over non-librating curved surfaces. Noir et al. (2009) and Noir et al. (2010) suggested that the Görtler vortices might exist in the molten cores of Earth's moon and Ganymede, in Callisto's subsurface ocean, molten cores of Mercury and Io, and in the subsurface oceans of Titan and Europa. In the current work, for the first time, it is tried to clarify the role of the Görtler vortices in generation of a zonal mean flow as a large scale motion in the bulk of a rotating cylinder with librating side walls.

The result might also contribute to our understanding of prograde and retrograde jets in the atmosphere. Development of the rotational instability due to an imbalance of forces has been studied in the meteorological context to understand the zonal mean flow generation; Griffiths (2003) investigated the nonlinear evolution of zonally symmetric *equatorial inertial instability*, Kloosterzeil et al. (2007) studied unfolding of the rotational instability in *initially barotropic vortices* in a uniformly rotating and stratified fluid using numerical simulation, Plougonven and Zeitlin (2009) investigated development of the inertial instability in a barotropic *parallel shear* (channel flow with horizontal shear) using the WRF model (Weather Research and Forecast mode). They concentrated on the development of instability which leads to a redistribution of angular momentum and make the system centrifugally stable. The new equilibrium state could be characterized by a redistribution of angular momentum and a resulting large scale motion as a mean flow. The concept mechanism of angular momentum transport into the stable environment, and the equation describing the final equilibrium state are still weakly understood. This work aims to close the gap.

Investigating the dynamics associated with formation of the large scale motion (upscaling of kinetic energy) requires a suitable approach which allows to capture the relevant scales of motion. A substantial increase of computational power over the last decade and proven adequacy of Navier-Stokes equations to model real phenomena in fluids encouraged the researchers to use numerical solution of Navier-Stokes equations to understand geo-and astrophysical fluid dynamics. Simulations resolving all relevant scales of motion are named Direct Numerical Simulation. They can be conducted for idealized configurations at Ekman numbers substantially larger than in atmosphere and ocean.

A rotating annular tank filled with a liquid is used in geophysical fluid dynamics community to study the atmosphere and ocean dynamics. We consider an isothermal homogenous fluid within a rotating annulus with walls partially subjected to longitudinal



libration and use direct numerical simulation to investigate the mechanisms 1 and 2. Longitudinal libration is considered to force the fluid flow. The configuration is idealized to isolate the effect of rotation. We exploit the different dynamical response of the fluid bulk to longitudinally librating lids and/or cylinder side walls in an axially closed and periodic annulus. Furthermore the impact of an inclination of the inner cylinder (frustum geometry) on the results is investigated. In principle, frustum resembles the upper half of near equatorial region of a sphere.

1.1 Objective

This thesis aims to contribute to the understanding of generation of the zonal mean flow in rotating fluids.

-We show that if the Stokes boundary layer becomes centrifugally unstable, the Görtler vortices are generated and propagate into the bulk due to the Coriolis effect and establish a zonal mean flow.

-First we show that inertial normal modes as global structures are able to generate a zonal mean flow via the nonlinear self interaction. Then we discuss that inertial waves (wave beams) as concentrated shear layers, which are generated by Ekman pumping and suction, are able to generate the normal modes efficiently. We show that inertial waves interact with the normal modes and affect generation of the zonal mean flow. Furthermore, we comment briefly on normal mode-boundary layer interaction and wave-wave interaction.

1.2 Outline

This study is arranged in two main parts based on the mechanisms 1 and 2 presented in section 1.1, and two additional parts for method, and summary and conclusion.

Chapter 2:

The governing equations in generalized curvilinear coordinates and the geometrical configurations are introduced. The spatial and temporal discretization, boundary conditions, and a convergence study for 2D (used in chapter 4) and 3D (used in chapter 3) direct numerical simulations are discussed as well. Note that the post-processing details of the numerical results are given in chapters 3 and 4.

Chapter 3:

The mean flow generation mechanism due to the Görtler vortices generated by a centrifugally unstable Stokes boundary layer is investigated using 3D-direct numerical simulation. A brief discussion of the centrifugal instability and the current status of understanding are given. Using longitudinal libration boundary conditions for either outer cylinder side wall and/or top and bottom lids, we show that the mean flow induced by the Görtler vortices affects the bulk flow likewise the flow driven by the nonlinearities in the oscillatory Ekman boundary layer. 3D-direct numerical simulations of the fluid flow in an

annular container with librating outer (inner) cylinder side wall, and Reynolds-averaged equations as diagnostic tools are used to investigate the generation mechanism of the retrograde (prograde) azimuthal mean flow in the bulk. We explain, phenomenologically, how the bulk angular momentum is mixed and homogenized due to propagation of the Görtler vortices, resulting in a new vortex of basin scale size. Then we investigate the Reynolds-averaged equations for the intermediate time scale of the development of the Görtler vortices, and for the long time scale of the order of several libration periods. Additionally, using the kinetic energy budget of fluctuating flow, the presence of an upscale cascade of energy is shown. The dependency of the azimuthal mean flow on Ekman number, libration amplitude and libration frequency are presented as well.

As last step in this chapter we present the azimuthal mean flow generation for an inclined inner wall annular container when the Stokes-Ekman boundary layer is unstable.

Chapter 4:

We consider low order inertial normal modes as standing waves and progressive inertial waves as concentrated beams in a rotating annular cavity with longitudinally librating top and bottom lids in a stable regime. The mean flow generation by the normal modes is investigated using the results of 2D-direct numerical simulations and analytical solution presented by Borcia and Harlander (2013). First, we show excitation of the normal modes in a viscous fluid, scanning the bulk kinetic energy close to the resonant frequency predicted by the analytical solution. Then following the procedure used by Tilgner (2007), the Navier-Stokes equations are segregated into linear and nonlinear parts at orders ε and ε^2 , respectively. The nonlinear equation is used to discuss generation mechanism of the mean flow. We discuss excitation efficiency of the mean flow by further decomposition of the velocity field into the wave beam and normal mode pattern. An analysis of libration phase difference between the wave beam and normal mode, in analogy to resonator and forcing in classical mechanics, allows us to explain the difference in excitation efficiency of the mean flow. Scaling behavior of the mean flow with respect to the Ekman number and libration amplitude is also given. Finally, we extend our work for the inner inclined wall annular container and show excitation of the normal mode and corresponding mean flow.

Chapter 5:

Summary, conclusion and suggestions for future studies are presented based on the results discussed in the chapters 3 and 4.



CHAPTER 2

GOVERNING EQUATIONS AND METHOD

2.1 Introduction

In this chapter, details of the governing equations and numerical solver are presented. First, governing equations in a co-rotating frame of reference and dimensionless parameters are introduced. Then the geometrical configurations and transformation relation into the generalized curvilinear coordinates are discussed in detail. We briefly touch the conservation properties of the numerical solver as well. Finally, details of the numerical solver, computations and code benchmark and numerical convergence study are given.

2.2 Governing Equations

We consider a homogeneous and incompressible fluid with kinematic viscosity ν bounded by two concentric cylinders (straight or inclined) and two end plates rotating about their symmetry axis, i.e. $\boldsymbol{\Omega}_0 = \Omega_0^* \mathbf{e}_z$ (see figure 2.1) where Ω_0^* is the mean rotation rate of the annulus (1/s). Inner cylinder radius is denoted by r_1^* , outer cylinder radius by r_2^* and height by H^* (in meter). To make the flow non-dimensional, compatible with system under investigation, the radius of the outer cylinder side wall is taken as length scale, and inverse of the mean rotation rate as time scale ($T^* = \Omega_0^{*-1}$). Consequently, $U^* = r_2^* \Omega_0^*$ and $p_0^* = r_2^{*2} \Omega_0^{*2}$ are velocity and pressure scales, respectively. Hence, non-dimensional quantities are given by:

$$u_i = u_i^*/U^*$$

$$p = p^*/p_0^*$$

$$r = r^*/r_2^*$$

$$z = z^*/r_2^*$$

$$\theta = \theta^*/r_2^*$$

$$t = t^*/T^*$$

where r , z and θ denote the dimensionless radial, axial and azimuthal coordinate directions, respectively and u_r , u_z , u_θ corresponding dimensionless velocity components, p denote dimensionless pressure and t dimensionless time.

The governing equations include the continuity and Navier-Stokes equations which are considered in a non-inertial frame of reference rotating with uniform angular velocity Ω_0^* about the vertical axis z . The non-dimensional Navier-Stokes and continuity equations in co-rotating frame of reference in Cartesian coordinates using vector notation are:

$$\begin{aligned} \frac{\partial \mathbf{V}}{\partial t} + (\mathbf{V} \cdot \nabla) \mathbf{V} + 2\mathbf{e}_z \times \mathbf{V} &= -\nabla P + E \nabla^2 \mathbf{V}, \\ \nabla \cdot \mathbf{V} &= 0, \end{aligned} \quad (2.1)$$

where \mathbf{V} is the velocity vector in the co-rotating frame of reference, P is the kinematic pressure taking into account centrifugal force, and E is the Ekman number representing the ratio of the viscous and the Coriolis forces, and is defined as

$$E = \frac{\nu}{\Omega_0 r_2^2}.$$

Wall libration is the only forcing mechanism present. In the laboratory frame of reference it is defined as

$$\Omega(t) = \Omega_0 [1 + \varepsilon \sin(\omega t)], \quad (2.2)$$

where ε is the dimensionless amplitude of the libration and ω is the dimensionless forcing frequency.

2.3 Geometrical configuration

At the equatorial part of a longitudinally librating solid spherical shell, since the tangent line to the sphere is parallel to the rotation axis, the boundary layer is similar to a Stokes boundary layer (Salon et al. 2011). In contrast, in the mid-latitude where the tangent line make an angle with respect to the rotation axis, the boundary layer is named oscillatory Stokes-Ekman boundary layer (Salon et al. 2011). This implies that the boundary layer has properties of both Ekman and Stokes boundary layer. The dynamical response of the fluid interior might differ for each of these two boundary layers. Using an annular tank with straight and/or inclined side wall, we are able to study the dynamical response of the fluid interior to Stokes, Ekman and Stokes–Ekman boundary layer. Stokes boundary layer is formed over the straight cylinder side walls which are parallel to the rotation axis. Oscillatory Ekman boundary layer forms over the top and bottom lids which are perpendicular to the rotation axis. In principle, inclined cylinder side wall resembles the upper half of near equatorial region of a sphere. According to the beta-plane approximation, vertical component of the rotation vector Ω_v incorporates into the Coriolis force and the contribution of the horizontal component Ω_H is supposed to be negligible, thus $f^* = 2\Omega \sin \alpha$; where α is inclination angle of the inner inclined wall cylinder (figure 2.1).

Straight and inclined wall annular configurations used in the present work are shown in figure 2.1. Inclined wall annulus is a truncated cone which is comprised of an inner inclined (frustum) and outer straight cylinder side walls (figure 2.1b). The tilted wall has an inclination angle $\alpha = 5.71^\circ$, and is designed using a Polynomial functions (Klien 2011, internal report). Dimensionless height denoted by H and inner and outer cylinder radii at the bottom by r_1 and r_2 , and r_3 radius of the truncated cone at the cylinder top. Details of the geometrical configurations used in chapter 3 and 4 are reported in table 2.1.

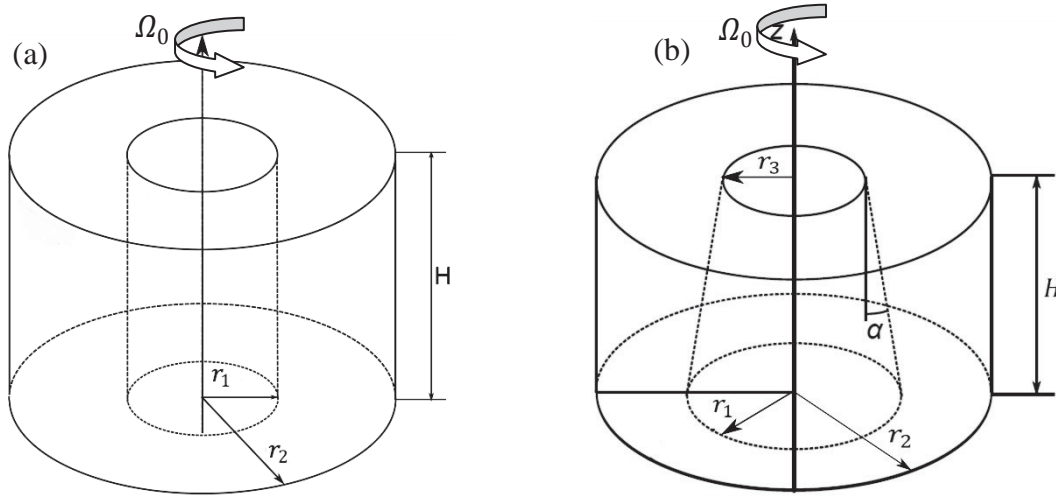


Figure 2.1: Schematic drawing of the straight (a) and inner inclined (b) wall annuli. Whole annulus rotates with the same angular velocity. Additionally, the boundaries liberate corresponding to the boundary conditions given in table 2.2.

Geometry	H	r_1	r_2	r_3	Thesis section
STR1	1.5	1.5	2.0	-	Chapter 3
STR2	1.5	1.0	2.0	-	Chapter 3
FRUS1	1.5	1.0	1.5	0.85	Chapter 3
STR3	3.0	1.0	3.0	-	Chapter 4
FRUS2	3.0	1.0	3.0	0.7	Chapter 4

Table 2.1: Details of the geometrical configurations. STR denotes the straight wall annulus (figure 2.1a) and FRUS the inner inclined wall annulus (figure 2.1b).

To solve the governing equations for the fluid flow within the two annular configurations, the governing equations are discretized in generalized curvilinear coordinates on a locally orthogonal grid. In the following t transformation relations are drafted.

2.4 Generalized curvilinear coordinates

One of the main problems of numerical simulation of the fluid flow in curved geometries is an accurate numerical representation of the boundary condition. This can be achieved when a coordinate line coincide with the curved boundary. An appropriate choice is

the generalized curvilinear coordinate system. We discuss, here, transformation relations between Cartesian and generalized curvilinear coordinate systems. Using these relations we arrive at the final form of the Navier-Stokes equations in curvilinear coordinate system which are solved numerically. If not stated else, the documentation is taken from the HYBRID-NEW code documentation Kaltenbach and will (2002) and Klein et al. (2014).

A curvilinear region in the physical space is mapped to a regular, rectangular region in computational space, where the mesh is uniform and Cartesian. This means that the mesh conforms to boundaries of the geometry. As a result, numerical techniques which are used in the Cartesian coordinate can be directly used to numerically solve the system of equations for the targeted curved geometry without any need for further modifications. However, to have numerically accurate solution, a particular attention must be paid to numerical discretization of the metric terms which map the physical grid into its counterpart in the computational space, and vice versa (Fletcher 1988).

In the following we present some basic of the mapping from physical Cartesian coordinates (y_1, y_2, y_3, t) to computational curvilinear coordinates (ξ^1, ξ^2, ξ^3, t) or (x^1, x^2, x^3, t) . Our goal is to write all terms in the Navier Stokes equations such that the independent variables are (ξ^1, ξ^2, ξ^3, t) or (x^1, x^2, x^3, t) . We start with transformation of gradient of any arbitrary field ψ from physical to computational space. Using the chain rule we obtain

$$\frac{\partial \psi}{\partial y_j} = \frac{\partial \xi^i}{\partial y_j} \frac{\partial \psi}{\partial \xi^i} \quad (2.3)$$

where

$$\vec{a}^i = \frac{\partial \xi^i}{\partial y_j} \vec{v}^j = \frac{1}{J} \gamma_j^i \vec{v}^j. \quad (2.4)$$

\vec{a}^i is contra-variant base vector normal to the surface formed by a pair of coordinate lines at a given point. A fundamental characteristic of curvilinear coordinates is existence of another set of base vectors which are tangent to the coordinate lines. They are called co-variant base vectors, and are given by

$$\vec{a}_i = \frac{\partial y_i}{\partial \xi^j} \vec{v}^j = c_j^i \vec{v}^j. \quad (2.5)$$

Components c_j^i form a 3×3 matrix which is the Jacobi matrix of transformation. Jacobian, J , is defined as the determinant of the Jacobian matrix. Usually, the components c_j^i are known but components γ_j^i are unknown. Our aim is to derive equation for the independent variables (ξ^1, ξ^2, ξ^3) . It is possible to compute γ_j^i from c_j^k , taking advantage of the fact that co- and contravariant are reciprocal bases ($\vec{a}_i \cdot \vec{a}^i = \delta_{i,j}$, where $\delta_{i,j}$ kronecker delta). One obtain (Thompson et al. 1985)



$$\gamma_j^i = \mathcal{J} g^{ik} c_k^j \quad (2.6)$$

$$g^{ik} = (g_{ki})^{-1} \quad (2.7)$$

where g_{ij} is co-variant metric components and g^{ji} contra-variant metric components. They are given by

$$\vec{a}_i \cdot \vec{a}_j = g_{ij} \quad (2.8)$$

$$\vec{a}^j \cdot \vec{a}^i = g^{ji} \quad (2.9)$$

Using γ_j^i , c_j^k and co- and contra-variant metric components, transformations from Cartesian to computational space, from co to contra-variant coordinates and vice versa can be given.

Transformation of velocity components

Contra-variant components of a velocity vector, which are derivatives of positions in computational space with respect to time, are given by

$$u^i = \frac{\partial x^i}{\partial t} = \frac{\partial x^i}{\partial y_j} \frac{\partial y_j}{\partial t} = \frac{1}{\mathcal{J}} \gamma_j^i v^j \quad (2.10)$$

where v^j represents velocity components in the Cartesian coordinate system. Cartesian components v^j can also be obtained from contra-variant velocity components u^i by the chain rule

$$v^i = \frac{\partial y_i}{\partial t} = \frac{\partial y_i}{\partial x^j} \frac{\partial x^j}{\partial t} = c_j^i u^j \quad (2.11)$$

Conservative and non-conservative derivative

Non-conservative derivative for a scalar quantity in generalized curvilinear coordinates for an arbitrary field ψ is given by

$$\frac{\partial \psi}{\partial y_i} = \frac{1}{\mathcal{J}} \gamma_j^i \frac{\partial \psi}{\partial x^j} \quad (2.12)$$

Derivative in conservative form can be expressed as

$$\frac{\partial \psi}{\partial y_i} = \frac{1}{\mathcal{J}} \frac{\partial}{\partial x^i} (\gamma_j^i \psi) \quad (2.13)$$

if